43rd Turbomachinery & 30th Pump Users Symposia (Pump & Turbo 2014)
September 23-25, 2014 | Houston, TX | pumpturbo.tamu.edu

REPETITIVE SHAFT CRACK FAILURE ANALYSIS ON A MULTISTAGE CENTRIFUGAL PUMP IN REACTOR CHARGE SERVICE IN A NUCLEAR POWER PLANT - BASED ON ODS AND FEA

Maki M. Onari
Manager of Turbomachinery Testing
Mechanical Solutions, Inc.
11 Apollo Drive
Whippany, New Jersey 07981, USA

Victor G. Arzani, P.E.
Principal Engineer
Duke Energy Corporation
4800 Concord Road
York, South Carolina 29745, USA

Maki M. Onari is a Principal Engineer and Manager of Turbomachinery Testing at Mechanical Solutions, Inc. (MSI), in Whippany, New Jersey, USA. He is responsible for field vibration testing involving ODS and Modal analysis. His career spans more than 18 years primarily working with rotating equipment analysis and troubleshooting in the petrochemical, refinery, and power generation industries. Prior to joining MSI, Mr. Onari was a Rotating Equipment Engineer in PDVSA-Venezuela responsible for the predictive maintenance of one of the largest petrochemical complexes in Latin America. Mr. Onari received his B.S degree (Mechanical Engineering, 1996) from the Zulia University in Venezuela. He is a member of ASME and the ISO TC108/S2 Standards Committee for Machinery Vibration.

Victor (Gerry) Arzani, P.E. is a Principal Engineer and Pump Engineer at Duke Energy Corporation in York, South Carolina, USA. He is currently serving as Pump Component Engineer for Duke's Nuclear Fleet. He provides leadership roles with PWR Owners Group, RCP working groups, and the Pump Users Group (formerly the EPRI PUG). Mr. Arzani dedicated his entire career with Duke Energy since 1981, including piping stress analysis, operations analysis group mostly vibration testing and analysis for the full fleet including Hydro, Fossil, Combustion Turbines and Nuclear facilities. Then 20 years at Catawba Nuclear Station as Predictive Maintenance Engineer. Mr. Arzani received his B.S degree (Mechanical Engineering, 1981) from NC State and holds his Masters in Engineering from University of South Carolina, 1989. In addition, Mr. Arzani obtained his Vibration Analyst Level IV in 1992 with Vibration Institute.

ABSTRACT

Two multistage barrel type pumps were installed in a nuclear power plant in reactor charge application. The pumps are driven by a 600 HP (447 kW) four-pole induction motor through double helical gear increasers. The overall vibration amplitude of the pump casing and the shaft were determined to be acceptable. However, one of the pumps was found with shaft repetitive cracking failures (MTBF = 7.3 years) initiated away from the key-way stress concentration area, under the later stage impellers, in a zone where fretting was occurring. Several attempts pursued by the plant and their supplier, over the years, did not find the root cause of this shaft cracking problem, in spite of the good troubleshooting procedures and careful installation practices pursued. Therefore, an exceptionally comprehensive root cause investigation was implemented, with specialty vibration testing at its core.

Thorough vibration testing combining spectral and time-transient vibration testing on the pump casing and shaft, Experimental Modal Analysis (EMA) testing of the impeller and pump casing, and Operating Deflection Shape (ODS) testing revealed the dynamic behavior of the pump rotor and the entire pump system. The results identified unsuspected excessive axial shuttling of the pump shaft at the motor running speed frequency due to axial run-out of the helical gear set. Based on the test results and supported by non-linear FEA analysis, the authors identified the root cause of the crack initiation phase of the shaft failure. An additional transient FEA based fracture mechanics analysis approach was able to predict that the stresses in the shaft, underneath the impeller, were able to encourage initiation and propagation of the crack.

This lecture demonstrates the effectiveness in machinery root cause investigations of thorough vibration testing including ODS, EMA, and FEA rather than traditional troubleshooting approaches, which had not detected a gear/pump inter-related problem, and would not have provided such clear visual evidence for decision makers.

INTRODUCTION

Acronyms

Description of the Pump

Two large turbine-generator Units were installed at Catawba Nuclear Plant (CNP), located in York, SC. The Units initiated their operation in 1985 and 1986 and were designed to generate 1200 MW per Unit. Each Unit was provided with two charge pumps designated as 1A/B NV and 2A/B NV for Units 1 and 2,

respectively. The charge pumps are centrifugal multistage (11 stages) barrel type pumps. These pumps were designed by Pacific Pumps (legacy pumps) model 2-1/2 RLIJ. The centrifugal Charging Pumps were originally specified as the high head safety injection pumps with capability as serving in alternate Charging / RCP (Reactor Coolant Pump) seal injection service in the Westinghouse NSSS (Nuclear Steam Supply System) ECCS (Emergency Core Cooling System) design. Many sites including Duke's Catawba and McGuire were not able to achieve the level of reliability with the positive displacement pumps desired and use these pumps for normal charging and RCP seal injection service. The common situation is two trains required operable, one always in service. For Catawba the normal charging / seal injection results in operation at 150 gpm (34.1 m^3/s), with B.E.P. at roughly 350 gpm (79.5 m^3/s) (43 percent of BEP) and run-out protection by system design and verified by system testing to limit flow to 560 gpm (127.2 m^3/s).

The pumps are driven by 600 HP (447 kW) electric induction motors operating at a constant speed of 1770 rpm (29.5 Hz) through a gear increaser at 4860 rpm output speed (81 Hz). The gear ratio is 1:2.746. All impellers were provided with 6 vanes and the diffusers with 8 vanes, rotating in the CCW direction as viewed from the suction end or drive end (DE).

Description of the Problem - Repetitive Crack Shaft Failure

The pump on which most of the testing was conducted was on the 1B NV, which was reported to be the only pump with three failures showing cracking at the discharge end of the shaft. The failures took place between 1989 and 2007 (MTBF=7.3 years). Figures 1 and 2 show the cross sectional drawing of these pumps and a photo of the problematic pump 1B NV.

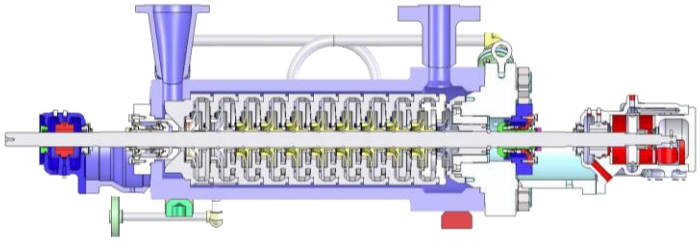

Figure 1. Charge Pump Cross-Sectional Drawing (Courtesy: Hydro-Aire, Inc.)

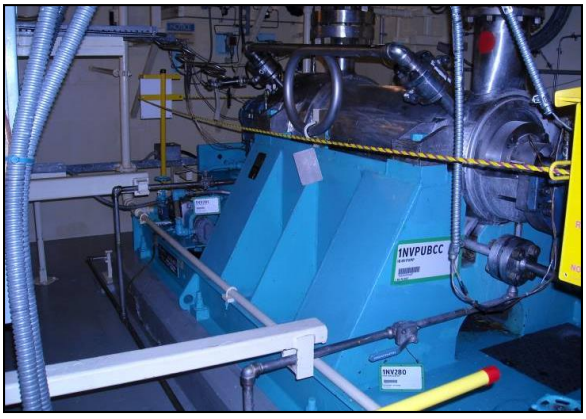

Figure 2. Photo of the 1B NV Pump

In 1989, the first failure took place, but the failure analysis was not properly documented and the failed shaft was not preserved. Three years later in 1999, a crack was found at the rear end of the 9th stage hub. In December 2007, the last failure was discovered under the 11th stage impeller hub (Figure 3) with evidence of fretting as shown in Figure 4. A circumferential crack was found at the keyway with 132 degrees arc as shown in Figure 5. It was also reported by CNP that the vibration amplitude of the pump had been always considered low and adequate.

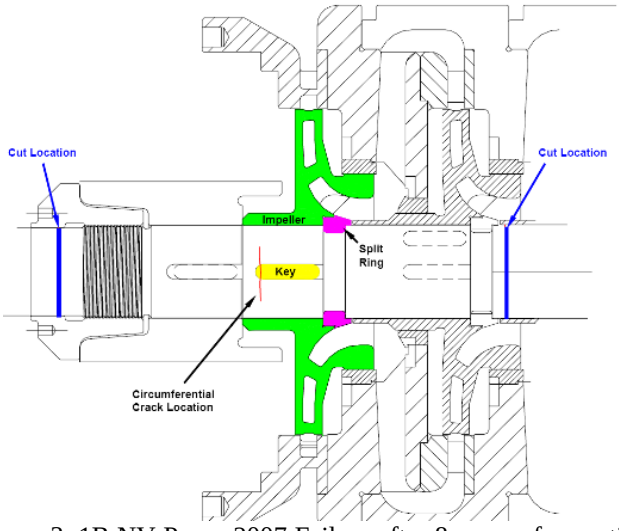

Figure 3. 1B NV Pump 2007 Failure after 8 years of operation. Crack Detected Under the 11th Stage Impeller hub

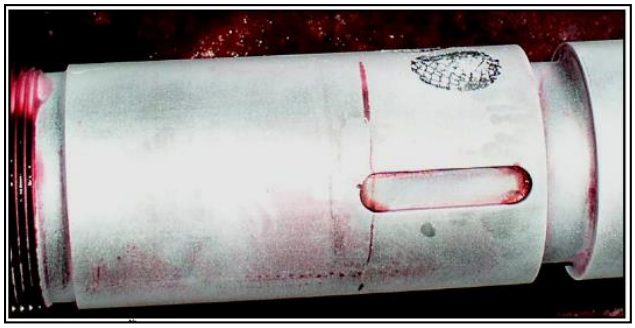

Figure 4. Detail of 11th Impeller Area with Circumferential Crack by Color-Contrast LPT. Redmond, 2008, Duke Power "Evaluation of CNS 1B NV Pump Shaft and Related Components – Metallurgy File #3917".

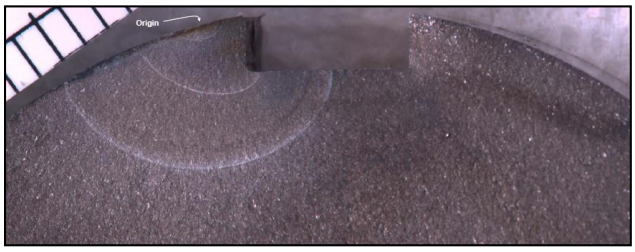

Figure 5. Fracture Overview Showing the Origin and the Crack Propagation. Redmond, 2008, Duke Power "Evaluation of CNS 1B NV Pump Shaft and Related Components – Metallurgy File #3917".

Table 1 shows a list of similar shaft crack failures that have been documented from different nuclear facilities around the country since their installation until 2007. The same charge pump design has had similar type of shaft crack failures and even complete fracture. The root cause of the failures in cells is likely related to the same issue described in this paper. However, further investigation should be conducted at those pumps/ facilities. Over the years numerous modifications have been implemented on these pumps in order to improve their reliability. Some of the changes are:

- Locknut threads that were concentrating the load on the first thread.
- Split ring failures developing cracks at the root of the split ring grooves (square groove profile to a cylindrical or continuously curved groove).
- Replacing the original Carbon Steel cladding casing to a Stainless Steel casing.
- Shaft material upgraded from original 414SS to CA-625 plus to improve its fatigue toughness.

Table 1. Data Base of Similar Shaft Failures of the Same Type of Pump/ Application Registered at Different Nuclear Sites within the US since their Installation until 2007

Nucler Site	Date	Failure	Location	Service Hours	Rotor Type	HP
DC Cook	Pre 1981	Shaft failure	Split Ring #4	5000	1969	600
DC Cook	Pre 1981	Shaft failure	Split Ring #11	5000	1969	600
DC Cook	Pre 1981	Shaft failure	Split Ring #2	10000	1969	600
Beaver Valley	Pre 1981	Shaft failure	Locknut threads	6500	1969	600
Beaver Valley	Pre 1981	Shaft failure	Locknut threads	6700	1969	600
Farley	Pre 1981	Shaft failure	Locknut threads	2500	1969	900
Zion	Sep-82	Complete fracture	Split Ring #11	1969	N/A	600
Farley	Mar-84	Complete fracture	Locknut threads	13483	1969	900
Beaver Valley	Dec-86	Complete fracture	Split Ring #2	15500	1972	600
Catawba	Jul-88	Cracked Shaft	Split Ring #11	8000	1972	600
Catawba	Nov-89	Bent Shaft	N/A	16000	1972	600
Sequoyah	Feb-91	Cracked Shaft	Under Impeller #11	30000	1969	600
Callaway	Feb-92	Complete fracture	Locknut threads	13000	1975	600
Harris	Mar-93	Complete fracture	Locknut threads	35000	1972	900
North Anna	Jul-93	Bent Shaft	N/A	19038	1969	900
DC Cook	Jul-93	Cracked Shaft	Under Impeller #9	26000	1969	600
Braidwood	Sep-93	Complete fracture	Under Impeller #10/11	1972	N/A	600
McGuire	Sep-93	Bent Shaft	N/A	45000	1972	600
Sequoyah	Jan-94	Complete fracture	Locknut threads	42000	1969	600
Sequoyah	Aug-94	Cracked Shaft	Under Impeller #1	50000	1969	600
Beaver Valley	Aug-94	Cracked Shaft	Under Impeller #11	20522	1969	600
Farley	1996	Complete fracture	Locknut threads	1969	N/A	900
Beaver Valley	1997	Complete fracture	Locknut threads	25000	1969	600
Sequoyah	Apr-99	Cracked Shaft	Under Impeller #11	15444	N/A	600
Catawba	Jun-99	Cracked Shaft	Under Impeller #9	40000	1985	600
Byron	2-Nov	Complete fracture	Split Ring #5	60000	1972	600
North Anna	3-Sep	Complete fracture	Split Ring #9	40000	1972	900
DC Cook	5-Jan	Cracked Shaft	Split Ring #11	16000	1993	600
Millstone	6-Jan	Complete fracture	Locknut threads	50000	1975	600
Catawba	7-Dec	Cracked Shaft	Under Impeller #11	36000	1993	600

Test Methodology

Typically pump OEM's and the End Users have used vibration data in order to diagnose and determine the root cause of any vibration-related issue by gathering a few readings from the bearing housings (in three orthogonal directions) and sometimes from the shaft (radial and axial displacement) both during steady and transient conditions of the pump. Approximately 90 percent of the cases of elevated vibration issues can be diagnosed using such a traditional approach from the bearing housings, and the solution can be implemented immediately (e.g. rotor imbalance, misalignment, bearing damage, etc.). However, the remaining 10 percent of pump vibration problems can be more subtle and lead to chronic reliability issues such as resonance, acoustic natural frequencies, premature wear of bushings and seals, bearing failures, structural cracks and looseness, coupling failures, rubbing, and even broken shafts. One of the more common of these difficult chronic problems is the synchronous excitation of structural natural frequencies, but unexpected problems can also occur due to sub-synchronous and super-synchronous problems. These result from rubs, fluid dynamic instabilities, recirculation, rotating stall, or structural resonances with high order excitation sources such as vane pass frequency.

Identifying the source of the problem requires a troubleshooting investigation that plant personnel can carry out if they are experienced. Alternatively they can be given appropriate guidance by the OEM or a qualified consultant that uses modern and high fidelity tools and approaches such as vibration data acquisition analyzers and computer simulation analysis software. The overall cost associated with this testing and analysis is considered negligible when compared to the expenditures for the continued rebuilding of damaged machinery components (repetitive failures) and associated downtime (i.e. over $1M/day of losses). Specifically, typical tools include vibration vs. time (wave forms), orbit plots, vibration vs. time trending, and vibration vs. frequency analysis (i.e. an FFT spectrum). In addition, higher level analysis exists such as Operating Deflection Shapes (ODS), Experimental Modal Analysis (EMA) or "bump" testing, combined with Finite Element Analysis (FEA). The ODS shows the relative motion in exaggerated fashion (amplitude and phase) of each portion of the structure at a given frequency. In this particular case, data for the Operating Deflection Shape (ODS) test was acquired at approximately 660 locations/ directions on the pump, gearbox, motor, pedestals, baseplate, and foundation. In addition, modal impact testing was performed on the 11th stage impeller (mounted on a stub shaft with slight press fit) to determine its natural frequencies and corresponding mode shapes (disk modes).

Pump 1B NV was the unit evaluated in detail by gathering vibration data at different flow capacities ranging from 145 gpm (32.9 m^3/h) to 160 gpm (36.3 m^3/h) [normal flow rate is 150 gpm (34.1 m^3/h), but the pumps are rated for 350 gpm (79.5 m^3/h). The vibration data from 1B NV was compared with its sister pump 2B NV from Unit 2 for comparison purposes.

INVESTIGATION

11th Stage Impeller Modal Test

Impact modal testing was performed on the actual impeller in order to determine its structural natural frequencies (disk modes) under dry and wet conditions. The impeller was mounted on a mandrel using the actual pressure fit of 0.5 mils diametral as shown in Figure 6. Figure 7 shows a photo of the impeller while performing the modal impact testing under wet condition, taking into account the added water mass effect, and impacting the eye in the axial direction.

The frequency response was measured using six mini single axis roving accelerometers. Figure 8 shows a computer model of the impeller indicating the locations where the measurements were taken. Typical Frequency Response Function (FRF) plots are shown in Figure 9 for the wet conditions. The list of natural frequencies of the impeller (disk modes) during the dry and wet conditions is shown in Table 2. Figure 10 shows the 2 Nodal Diameter (2ND) mode shape at 2620 Hz under dry conditions. Figure 11 depicts the Interference Diagram of the impeller indicating the first family of modes (dry).

Based on this test, it was concluded that the construction of the impeller was robust enough that its natural frequencies or disk modes were well above potential excitation sources in regards to the number of rotating vanes (6 vanes) and diffuser vanes (8 vanes). In this case the main excitation shape would be at 2 Nodal-Diameter (2ND), which is the difference between the number of diffuser vanes and the impeller vanes.

Figure 6. 11th Stage Impeller Mounted on a Mandrel

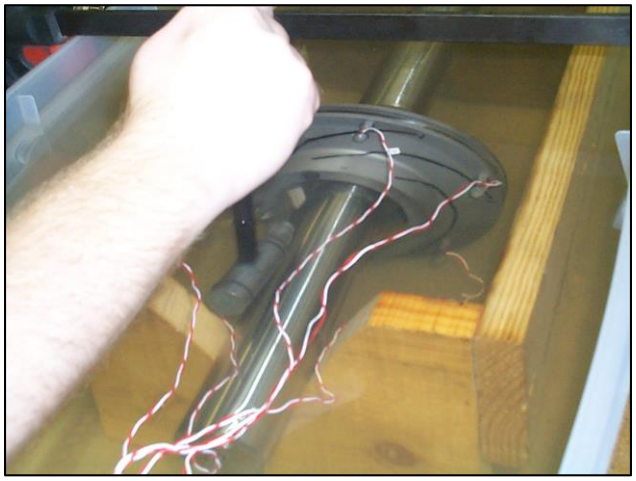

Figure 7. Experimental Modal Analysis Test of the 11th Stage Impeller Wet Conditions

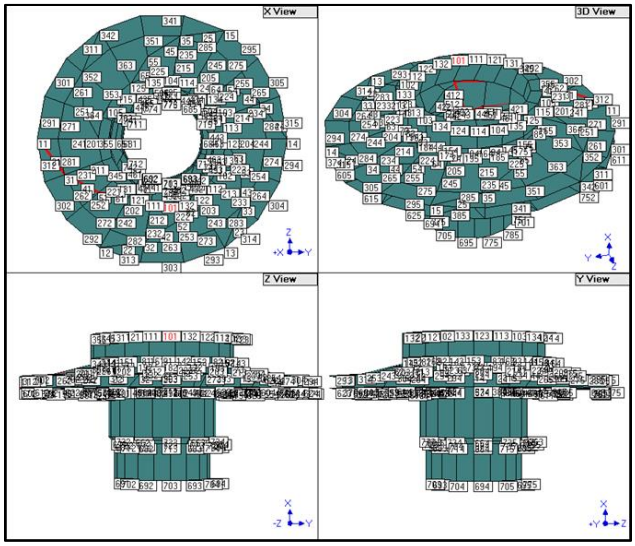

Figure 8. Computer Model of the Impeller. Each Label Represents a Measurement Location

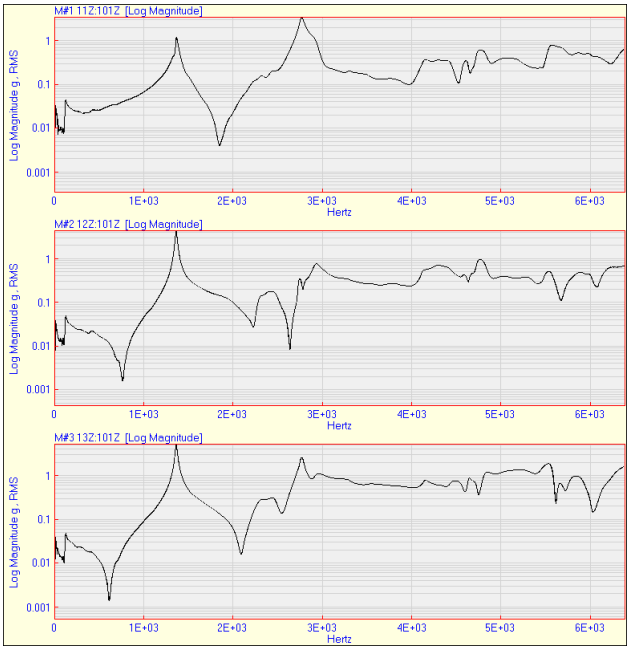

Figure 9. Typical Frequency Response Function (FRF) Spectra Under Wet Conditions

Table 2. List Natural Frequencies of the Impeller (disk modes) During the Dry and Wet Conditions

Mode Shape Description	Natural Frequency Dry Condition (Hz)	Natural Frequency Wet Condition (Hz)
0 Nodal Diameter "Umbrella" Mode	3510	3420
1 Nodal Diameter 0 Nodal Circle	1550	1360
2 Nodal Diameter 0 Nodal Circle	2620	-
2 Nodal Diameter 0 Nodal Circle	3310	2770
3 Nodal Diameter 0 Nodal Circle	5320	4630

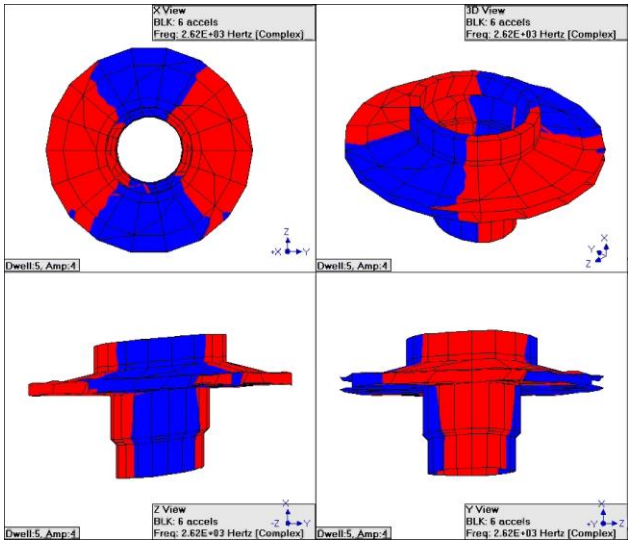

Figure 10. Mode Shape at 2620 Hz (2ND Mode)

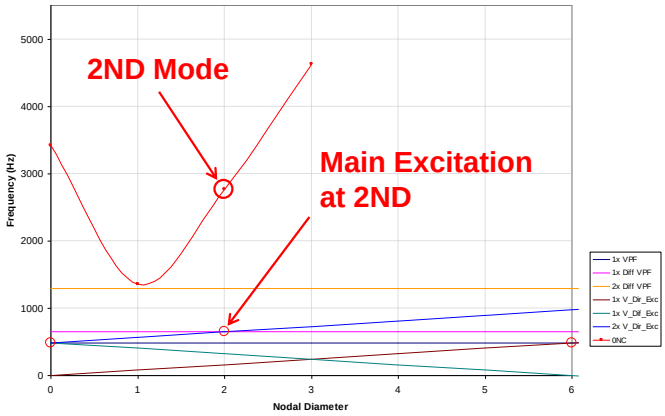

Figure 11. Interference Diagram under Dry Conditions

Specialized Field Vibration Testing

1B NV Pump EMA Test

The outboard bearing (OBB) housing was impacted in the axial direction and the frequency response was recorded using an axial proximity probe installed in the same direction as shown in Figure 12.

Figure 12. EMA Test at the OBB in the Axial Direction Using a 3 lbm Hammer

The Time Averaged Pulse (TAP™) technique was used to take into account the operating fluid film stiffness for the thrust bearing. This test was performed with the pump operating at 145 gpm (32.9 m^3/h) to determine if there are any potentially relevant axial natural frequencies of the pump shaft. After several hundred impacts, the final FRF plot (Figure 13) did not indicate any natural frequency in the vicinity of the running speed of the pump (81 Hz). In contrary, a strong excitation at the motor running speed was observed (29.5 Hz). The only natural frequency identified was at approximately 121 Hz. However, this natural frequency is difficult to be excited. The 4x rpm of the motor is the closest harmonic and it is considered a weak excitation source, especially in the axial direction. The same test was performed while the pump was operating at 160 gpm (36.3 m^3/h) of capacity indicating a similar frequency response.

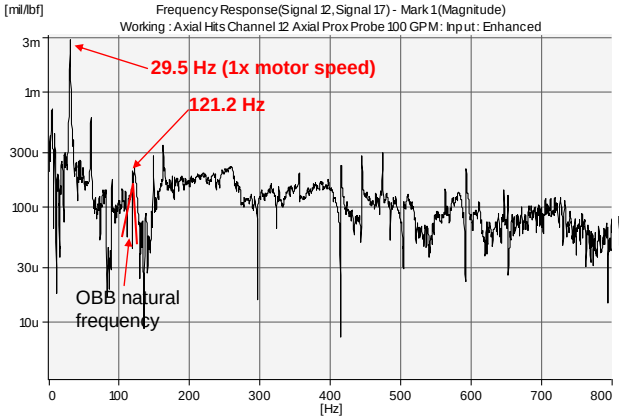

Figure 13. 1B NV Pump EMA Test - FRF Plot from the Axial Proximity Probe at the OBB (mil/lbf versus Frequency in Hz)

2B NV Pump EMA Test

Modal impact testing performed on the counterpart pump from Unit 2 was conducted while it was operating at 160 gpm of capacity to determine if any potential axial natural frequencies of the shaft could be detected by reading the frequency response from the permanently installed axial proximity probe. After several hundred impacts, the final FRF plot, shown in Figure 14, did not indicate any natural frequency in the vicinity of the running speed of the pump. In this particular pump, the strongest excitation was detected at the running speed of the pump, which was expected. The motor speed excitation was not present. In addition, the same structural natural frequency was detected at 118 Hz. Similarly, this mode can be excited by the 4th harmonic of the motor running speed, which was considered weak and unlikely.

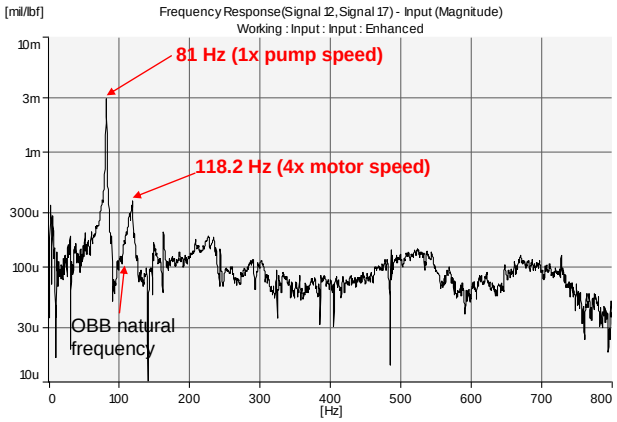

Figure 14. 2B NV Pump EMA Test - FRF Plot from the Axial Proximity Probe at the OBB (mil/lbf versus Frequency in Hz)

Continuous Monitoring Test 1B NV & 2B NV

During normal operation of the 1B NV pump at 145 gpm (32.9 m^3/h) or (85 gpm [19.3 m^3/h] + 60 gpm [13.6 m^3/h] of min-flow) the pump indicated a relatively low vibration level of 0.15 in/s pk (3.8 mm/s pk) at the running speed of the pump or 81 Hz measured at the OBB housing in the vertical direction as can be seen in the vibration spectrum in Figure 15. Notice the broadband peak indicating a structural natural frequency of the OBB housing at approximately 120 Hz.

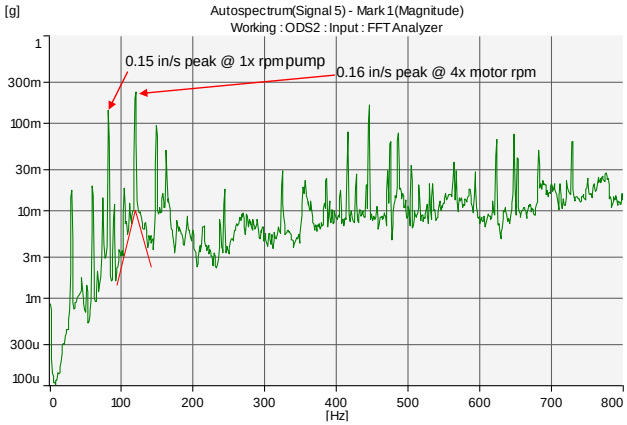

Figure 15. 1B NV Pump Vibration Spectrum at the OBB in the Vertical Direction (g's versus Frequency in Hz)

In contrast to the 1B NV pump, vibration readings taken from the 2B NV pump indicated different behavior from a dynamic stand point. This pump was tested only at 160 gpm (100 gpm [22.7 m^3/h] + 60 gpm min-flow [13.6 m^3/h]). The maximum discrete vibration at steady-state conditions at the running speed frequency was measured at the OB bearing housing in the same vertical direction (0.06 in/s or 0.15 mm/s) pk, which was considered low (Figure 16). A similar natural frequency was observed near 120 Hz.

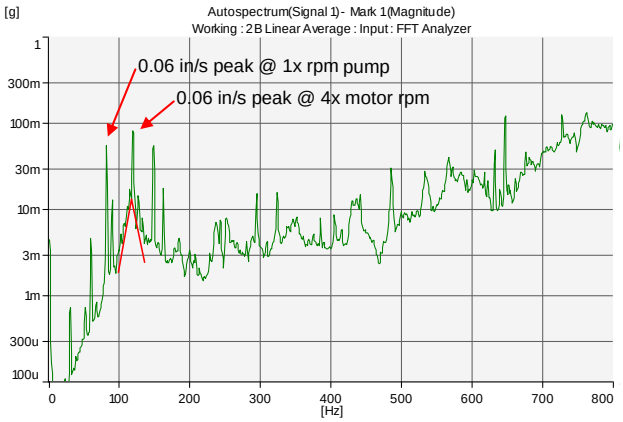

Figure 16. 2B NV Pump Vibration Spectrum at the OBB in the Vertical Direction (g's versus Frequency in Hz)

The axial proximity probe installed at the OBB of the 1B NV pump indicated an interesting narrow band peak at approximately 30 Hz, which represented the running speed of the motor. The amplitude of this spike was measured to be almost 0.5 mils pk-pk (12.7 microns pk-pk). Figures 17 and 18 show the FFT and the time waveform plots from the axial probe, respectively. CNP had reported that the axial motion of this pump had been detected as high as 1.7 mils (43.2 microns) pk-pk, while the other three charge pumps only showed mostly displacement at the running speed of the pump (81 Hz) likely due primarily to mechanical axial run-out of the target plate of the probe.

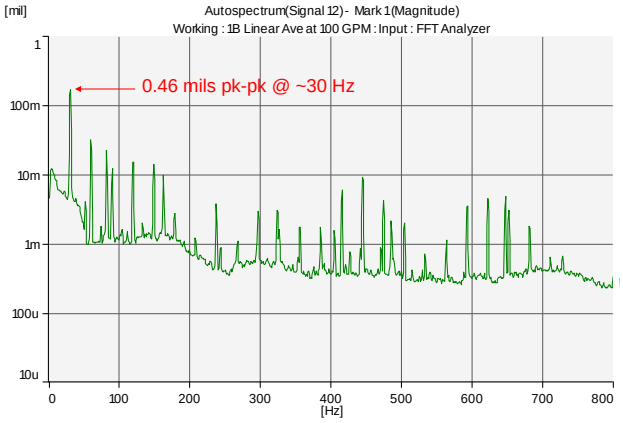

Figure 17. 1B NV Pump Axial Proximity Probe Vibration Spectrum (mils rms versus Frequency in Hz)

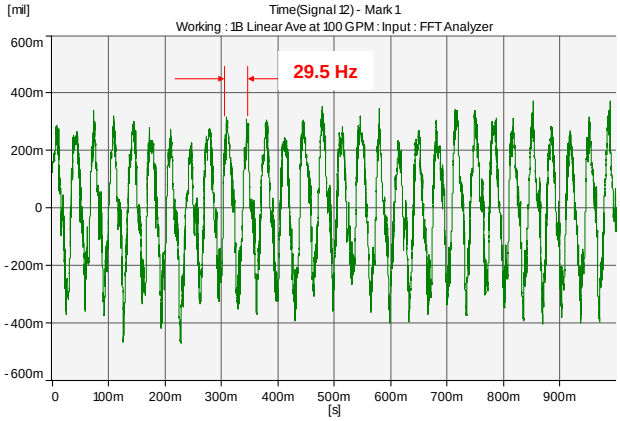

Figure 18. 1B NV Pump Axial Proximity Probe Vibration Waveform (mils versus Time in Seconds)

Vibration reading from the axial proximity probe installed at the OBB of the 2B NV pump indicated 12 times smaller amplitude (0.04 mils or 1.0 micron) pk-pk at approximately 30 Hz, when compared with the 1B NV pump. The highest amplitude was measured to be only 0.4 mils (10.2 micron) pk-pk at the running speed of the pump, which was expected, but mostly due to axial run-out of the target surface. Figures 19 and 20 depict the FFT and the time waveform plots from this axial probe, respectively, indicating the amplitude and the frequency of this axial motion of the 2B NV pump shaft.

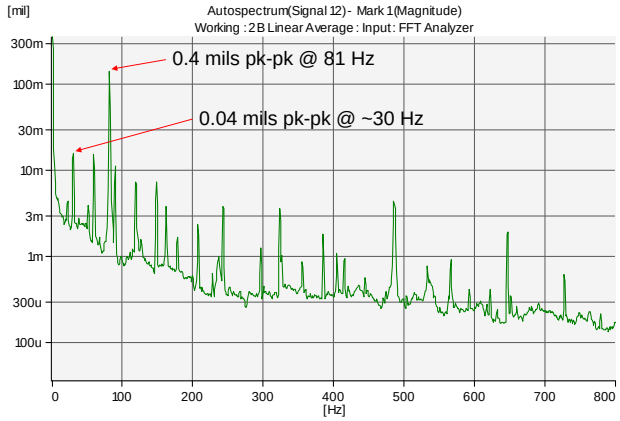

Figure 19. 2B NV Pump Axial Proximity Probe Vibration Spectrum (mils rms versus Frequency in Hz)

The rotor motion was monitored via permanently installed radial proximity probes. The rotor vibration levels on both pumps were on the order of 1.3 and 2.1 mils (33.0 to 53.3 microns) pk-pk measured at the OBB and IBB at 1x rpm of the pump, respectively, which were considered acceptable for this type of machine.

Dynamic pressure measurements were taken on the 1B NV pump suction, discharge, and the balance line. All taps were bled free of air prior to startup, and very little air build-up was observed. Pressure pulsations and their acoustic natural frequencies did not indicate evidence or correlation with previous failures of the pump shaft.

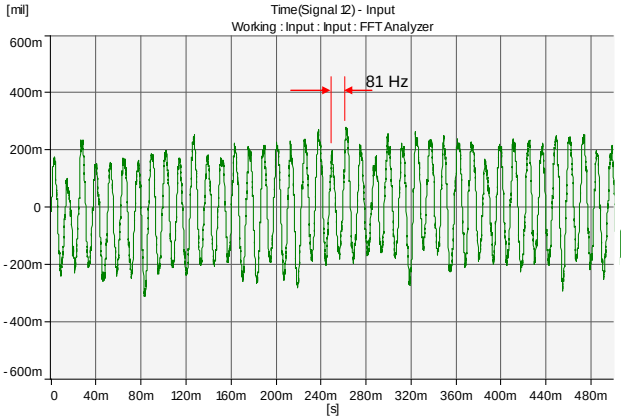

Figure 20. 2B NV Pump Axial Proximity Probe Vibration Waveform (mils versus Time in Seconds)

Operating Deflection Shape (ODS) Testing

Detailed ODS testing was conducted on both pumps for comparison purposes. Figure 21 shows a 3D CAD computer model used to create animations of the pump structure at its main excitation sources (i.e. 1x rpm of the motor, 1x rpm of the pump, etc.).

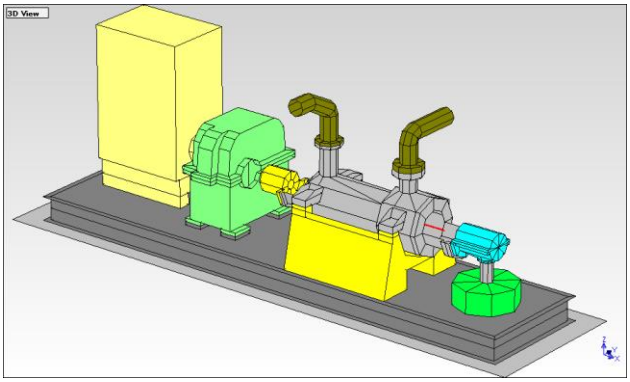

Figure 21. Charge Pump CAD Computer 3D Model for ODS Testing

Figure 22 shows the same CAD computer model of the pump system assigning motion to each individual vibration data point. Each label represents the location where a tri-axial accelerometer was placed (roving accelerometers) in order to characterize the overall global relative motion of the pump at a given frequency. Over 700 vibration locations / directions were recorded to create a data base of amplitude versus frequency and phase angle.

1B NV Pump ODS Testing

The ODS animation at 1x rpm of the motor (30 Hz), which is shown in Figure 23, indicated relatively high axial motion of the pump shaft driving the vertical rocking motion of the OBB (in-phase motion). The gearbox also shows axial rocking motion in phase with the pump shaft motion. At the running speed of the pump (81 Hz), the animation shown in Figure 24 indicated an orbiting motion of the OBB along with a typical radial motion of the pump shaft, while the rest of the unit remained stationary.

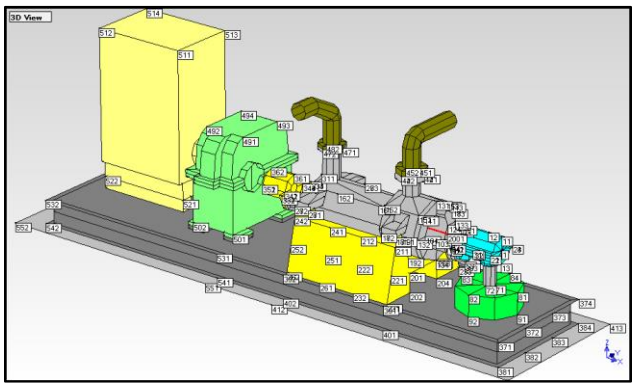

Figure 22. Charge Pump CAD Computer 3D Model for ODS Testing Tri-axial Accelerometer Locations

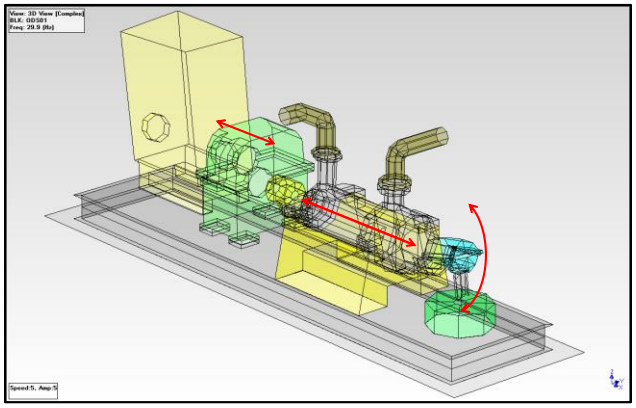

Figure 23. 1B NV Pump ODS at 1x rpm of the Motor (30 Hz)

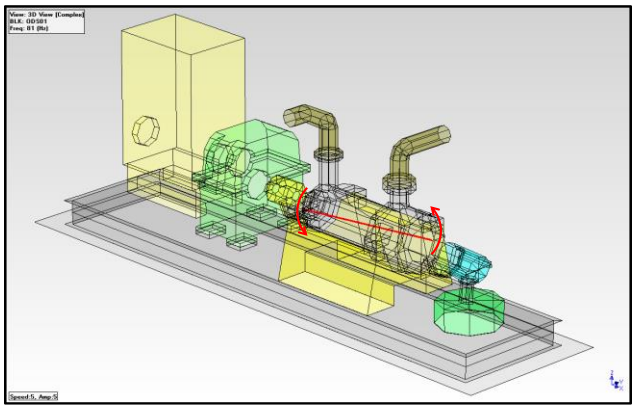

Figure 24. 1B NV Pump ODS at 1x rpm of the Pump (81 Hz)

2B NV Pump ODS Testing

The ODS animation at 1x rpm of the motor is shown in Figure 25. In contrast to the offending pump, at this frequency the motor indicated rocking motion in the axial direction. The rest of the unit remained basically stationary (without axial motion of the pump shaft). The ODS animation at the running speed of the pump, shown in Figure 26, described typical orbiting motion of the pump shaft.

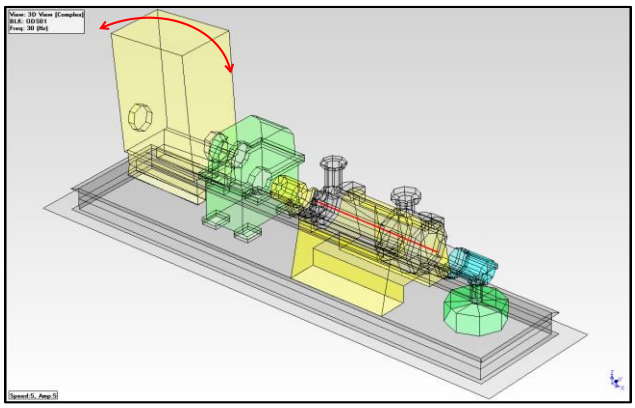

Figure 25. 1B NV Pump ODS at 1x rpm of the Motor (30 Hz)

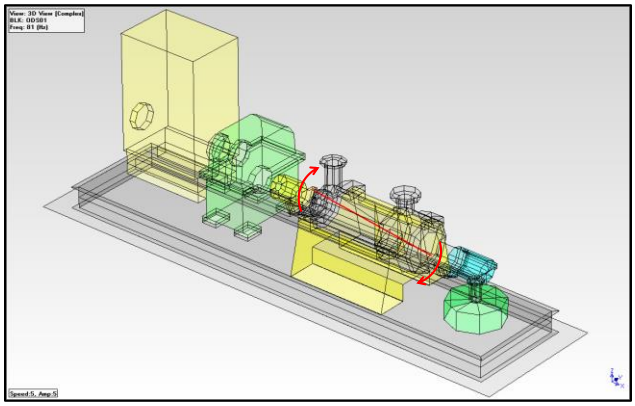

Figure 26. 1B NV Pump ODS at 1x rpm of the Pump (81 Hz)

Based on dynamic data gathered, there was no evidence of any natural frequency in the axial direction to amplify the axial vibration at the running speed of the motor. Therefore, it was concluded that the most likely root cause of the repetitive crack initiation of the pump shaft was due to fretting and/ or wear marks observed between the impeller hub and the shaft while the pump shaft was oscillating axially, reacting against the hydraulic thrust load depending on the operating point of the pump. The crack propagation that was associated with the high-cycle fatigue process was investigated later on using an FEA-based fracture mechanics approach. The elevated oscillating motion of the pump shaft, at the running speed of the motor (30 Hz), was attributed to one of the following causes:

- Axial motion of the motor shaft due to operation off its magnetic center.
- Misalignment between the motor and the gearbox leading to axial run-out.
- Axial mismatch between the helical gears (apex) acting as axial run-out.

In general, the axial force of the motor rotor out of its magnetic center is not considered strong enough to sufficiently move the pump shaft. Any axial run-out due to the coupling would have been identified during the alignment process between the motor and the gearbox. Therefore, potential axial mismatch of the helical gear set was considered as the most likely cause of the axial displacement of the pump shaft at the driver's operating speed. This would generate an impulsive displacement load (non-sinusoidal waveform) due to a geometric abnormality of

the gear teeth of the input shaft (axial run-out). In addition to this, the apparently rigidly behaving gear coupling between the gearbox and the pump was not absorbing this axial motion as it should. Note that this gearbox and the couplings have been installed since the initial start-up of the unit in 1986 and have not been replaced.

Finite Element Analysis (FEA)

Non-Linear Transient Dynamic Contact Analysis

An axi-symmetric model of the pump rotor assembly was idealized to include the shaft and the last stage impeller of the pump (11th stage) as shown in Figure 27. Plane type elements were used resulting in roughly 28,000 degrees of freedom FEA break-up (Figure 28). The model was run using transient dynamic solution techniques.

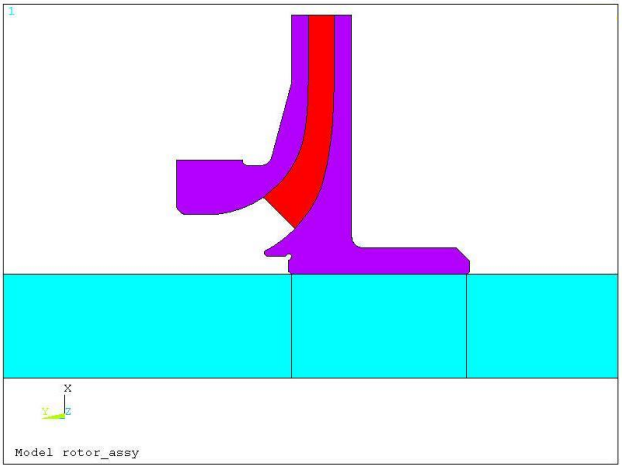

Figure 27. Axi-Symmetric Model of the 11th Stage Impeller and Shaft Assembly

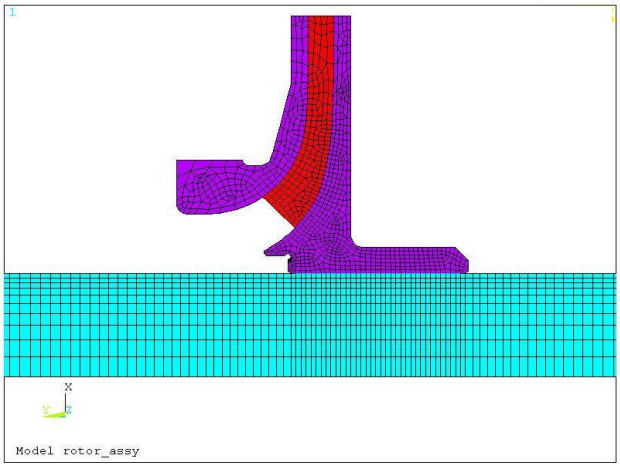

Figure 28. Axi-Symmetric Break-Up Model of the 11th Stage Impeller and Shaft Assembly

Note that the impellers blading was simulated with axisymmetric elements by using an orthotropic material with the proper average density and stiffness within the impeller blade zone.

A 75 psi (5.2 bar) pressure saw-tooth impulse of 0.2msec duration was applied to the inboard end of the shaft. This impulse was determined to result in 30 g (294.2 m/s^2) acceleration at the outboard end, which correlated with the axial proximity probe readings. Figures 17 and 18 show the vibration spectrum and wave form from the axial proximity probe mounted at the outboard bearing of the pump. Figure 29 depicts the acceleration differentiated two times from the proximity probe displacement data.

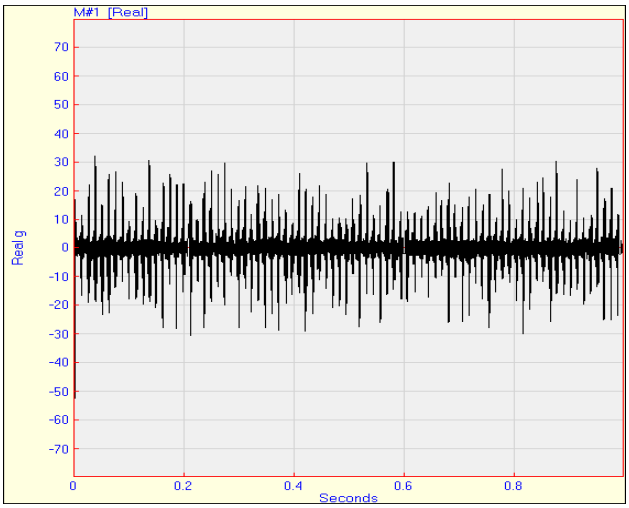

Figure 29 Acceleration Signal Derived From Axial Proximity Probe Readings (g's versus Time in Seconds)

The FEA model was loaded using the following load steps:

- Load Step 1: Initiate and complete the interference fit between the impeller and the shaft (2 mils or 50.8 microns of diametral interference) and constrain the OB end of shaft at the thrust bearing
- Load Step 2: Ramp-up an axially applied pressure of 75 psi (5.2 bar) load to the inboard end over in 1.0msec (30 g's pk or 294.2 m/s^2 pk acceleration).
- Load Step 3: Ramp pressure down to a 0 psi (0 bar) over an additional 0.1msec.
- Load Step 4: Run for an additional 1.0msec to monitor the traveling of the acoustic waves and the impeller interface conditions.

Based on the transient dynamic analysis it revealed that acoustic wave propagation in the shaft was able to result in micro-motion at the press fit interfaces. Therefore, the idealized axi-symmetric model of the pump shaft and the last stage impeller predicted that a momentary sliding condition exists between the impeller and the shaft. This sliding condition led to fretting damage and crack initiation. Figure 30 shows a contact status plot between the impeller hub and the shaft at load step 4. Red zones indicate sticking and orange areas means sliding status. Therefore, most of the contact area indicated sliding effect under 30 g's (294.2 m/s^2) pseudo-static loading of "jerk" effect.

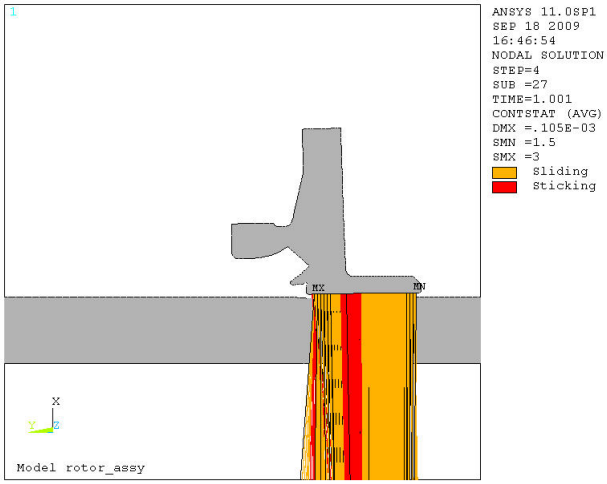

Figure 30 Contact Status Plot at Load Step 4

FEA-Based Fracture Mechanics Approach

Once it was demonstrated that the fretting was the cause of crack initiation, it was demonstrated that the crack can be propagated into the shaft using FEA and fracture mechanics approach. This analysis assumed that relative sliding velocity between the impeller and shaft was equivalent to the peak axial shaft velocity measured at the OB end of shaft near the thrust bearing. It also assumed that fretting condition and asperities on the shaft surface caused the impeller to axially lock-up against the shaft. The lock-up behavior was modeled as an axial impact between the shaft and impeller in the region of the assumed 5.0 mils deep (127 microns) crack (underneath the impeller hub). Transient dynamic FEA technique was used to predict the stress distribution near the crack and calculate the stress intensity factor. This stress intensity factor (based on output form the FEA program) was used to compare against the crack-growth rate of the shaft material.

Figure 31 shows the same axi-symmetric model with a finer break-up around the initial crack (5.0 mils or 127 microns) included into the model. Figure 32 shows a zoomed view of the explicitly modeled crack on the shaft.

Figure 33 shows von Mises stress plot (psi) calculated by the FEA program at the root of the crack during the impact event ("jerk" effect). Note that the double peak observed is due to flexing of the impeller and later spring-back response. The stress distribution (von Mises) in the vicinity of the crack (psi) is shown in Figure 34.

The stress-intensity factor (ΔK_I) was calculated to be 16.3 ksi$\sqrt{in}$ (17.9 MPa$\sqrt{m}$). Based on the experimental crack-growth rate graph of a similar material (Figure 35) in water at 2400 cpm, the calculated stress-intensity-factor intersected the curve beyond the threshold point. Therefore, crack propagation was expected to occur.

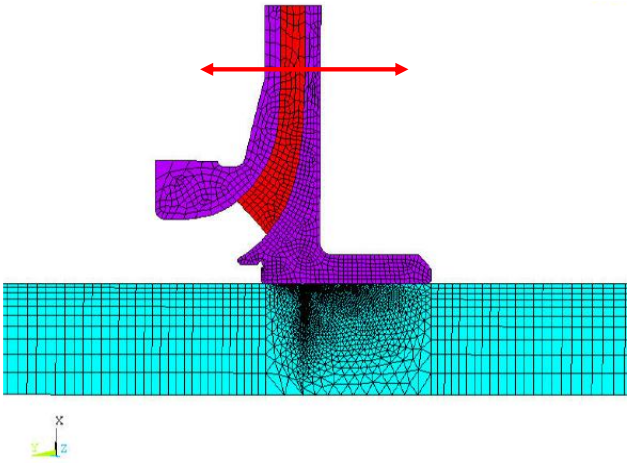
Figure 31 Impact Acceleration of 30 g's pk (294.2 m/s^2) at 30 Hz

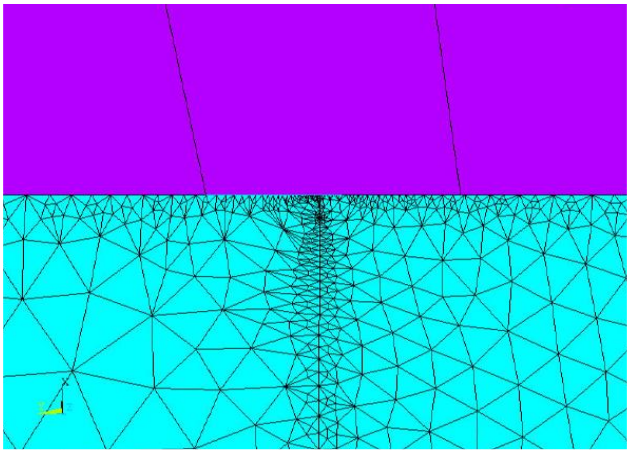
Figure 32 Explicitly Modeled 0.005 inch (127 microns) Crack on the Shaft

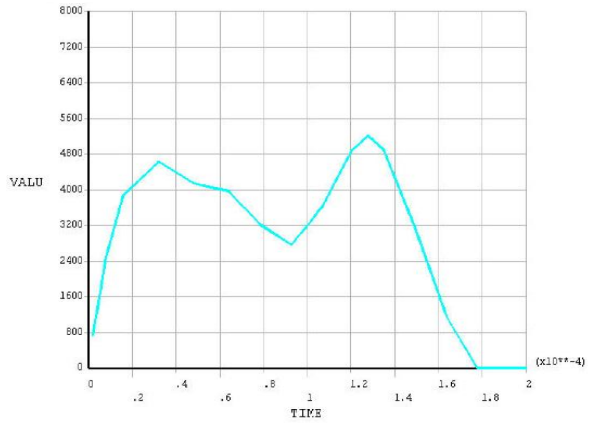

Figure 33 von Mises Stress Plot (psi) at Root of Crack

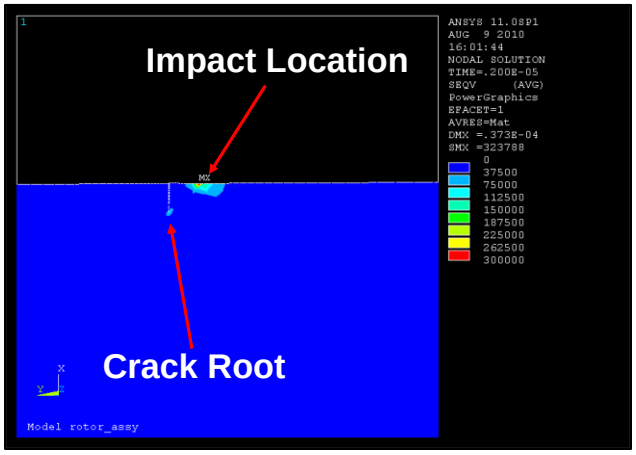

Figure 34 von Mises Stress Contour Plot (psi) in the Vicinity of the Crack

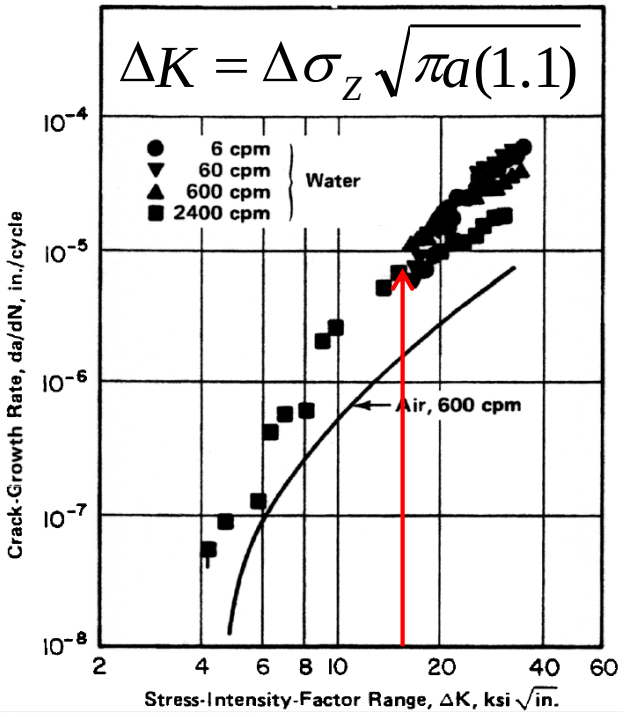

Figure 35. Crack-Growth Rate versus Stress-Intensity-Factor Range for 403SS. (Source: Aerospace Structural Metals Handbook). ΔK is the stress intensity factor, $\Delta\sigma_Z$ is the stress range perpendicular to the to the crack or flaw, and a is the length of the crack or initial flaw.

CONCLUSIONS AND RECOMMENDATIONS

- The root cause of the repetitive cracking of the pump shaft was due to a fatigue process while the pump shaft was oscillating axially driven by the gear tooth circumferential run-out.
- The axial mismatch of the helical gear set (apex) was the cause of the axial displacement of the pump shaft at the driver's operating speed, generating an impulsive displacement load due to a geometric abnormality of the gear teeth of the input shaft gear (~7 mils [178 microns] of axial run-out).
- The ODS test performed on 1B NV Pump, at the running speed of the motor (30 Hz), indicated significant axial motion of the pump shaft at the motor running speed driving the OBB with a vertical rocking motion. The gearbox casing moved axially with some phase lag with respect to the pump shaft and the motor casing. The vibration test performed on 2B NV Pump did not indicate any abnormal axial motion of the pump shaft at the running speed of the motor (0.04 mils [1.0 micron] pk-pk versus 0.5 mils [12.7 microns] pk-pk measured on 1B NV Pump).
- Traditional troubleshooting approaches probably would not have indicated a gear/pump inter-related problem, and would not have provided such clear visual evidence for decision makers.
- ODS & EMA testing, coupled with appropriate analysis, are powerful troubleshooting tools to facilitate and visually understand the most difficult vibration problems in turbomachinery and pumping systems.
- The gearbox on 1B NV pump was recommended to be refurbished by replacing the gear set. In addition, was suggested to verify the actual axial run-out of the output shaft by turning the input shaft. This action was accomplished in 2010 and it was found that the axial run-out of the output shaft was measured to be approximately 7 mils (178 microns).
- The couplings between the pump and the gearbox as well as between the gearbox and the pump were also recommended to be replaced. This action item was implemented in 2010.

REFERENCES

Blevins, Robert D. Ph.D., 1979, "Formulas for Natural Frequency and Mode Shape," Reprint Edition 2001, Van Nostrand Reinhold Company, Inc, New York, USA.

Bowman, D., Marscher, W., and Reid, S., 1990, "Pump Rotor Critical Speeds: Diagnosis and Solutions," *Proceedings of International Pump Users Symposium*, Texas A&M University.

Brown, W.F., 1998, "Aerospace Structural Metals Handbook," Volume 2, CINDAS/USAF CRDA Handbooks Operation, Purdue University, West Lafayette, IN.

Ewins, D. J. 1984, "Modal Testing: Theory and Practice" *Research Studies Press LTD.*, Taunton, Somerset, England.

Lienau, W. and Lagas, N., 2008, "Evaluation of Rotordynamic Criteria for Multistage Pump Shafts," *Proceedings of International Pump Users Symposium*, Texas A&M University.

Marscher, W. D., Boyadjis, P. A, Onari, M. M., Cronin, R. J., Kelly, W. J., Olson, E. J., and Gaydon, M. A., 2008, "*Centrifugal Pump Mechanical Behavior and Vibration* Chapter," *Pump Handbook*, 4th Edition, Ed. Karassik, I. J., Messina, J. P., Cooper, P., and Heald, C. C., McGraw-Hill, New York, NY, USA.

Marscher, W. D., 1986, "Determination of Pump Rotor Critical Speeds During Operation Through Use of Modal Analysis," *Proceedings of ASME WAM Symposium on Troubleshooting Methods and Technology*, Anaheim Cal.

Marscher, W. D., 1989, "Analysis and Test of Multistage Pump Wet Critical Speeds," *ASLE/ASME Joint Tribology Conf*., Ft. Lauderdale, Florida, USA

Marscher, W. D. and Jen, C-W, 1990, "Using Time-Averaged Modal Excitation to Determine the Rotor Dynamic Bearing Coefficients of Centrifugal Pumps," *Proceedings of 8th International Modal Analysis Conference*, Kissimmee, Florida, USA

Marscher, W. D., 1991, "How to Use Impact Testing to Solve Pump Vibration Problems," *Proceedings EPRI Power Plant Pumps Symposium*, Tampa, Florida, USA.

Marscher, W. D., 1997, "Rotating Machinery Vibration and Condition Monitoring," *Chapter of Tribology Data Handbook*, CRC Press, Boca Raton, Florida, USA, pp. 944-955.

Marscher, W. D., 1999, "The Determination of Rotor Critical Speeds While Machinery Remains Operating through Use of Impact Testing", *IMAC Conf.* Orlando Florida.

McConnell, K. G., 1995, "Vibration Testing Theory and Practice," John Wiley & Sons, Inc., New York, NY, USA.

Onari, M. M. and Boyadjis, P. A., 2009, "Solving Structural Vibration Problems Using Operating Deflection Shape (ODS) and FEA," *Proceedings of 25th International Pump Users Symposium*, Texas A&M University.

Onari, M. M. and Olson, E. J., 2008, "Solving Structural Vibration Problems Using ODS Analysis," *Proceedings of 37th Turbomachinery Symposium*, Texas A&M University.

Redmond, K., P.E., 2008, "Evaluation of CNS 1B NV Pump Shaft and Related Components – Metallurgy File #3917," *Duke Power – Nuclear Generation – Materials Engineering & Lab Services*, Huntersville, North Carolina. pp. 8-18.

Stavale, A. E., 2008, "Reducing Reliability Incidents and Improving Meantime Between Repair," *Proceedings of International Pump Users Symposium*, Texas A&M University.

Thomson, W. T. and Dahleh M. D., 1993, "Theory of Vibration with Applications," Fifth Edition, Prentice-Hall, Inc, Upper Saddle River, New Jersey, USA.